

Anomalous Heat Effects by Interaction of Nano-Metals and H(D)-Gas

**A. Takahashi^{*1,3}, A. Kitamura^{1,2}, K. Takahashi¹, R. Seto¹,
T. Yokose², A. Taniike² and Y. Furuyama²**

¹Technova Inc., Chiyoda-ku, Tokyo, 100-0011 Japan,

² Kobe University, Graduate School of Maritime Science, Kobe, 658-0022 Japan

³ Osaka University, Suita, Osaka, 565-0871 Japan

*akito@sutv.zaq.ne.jp

[Abstract]

Brief review of Technova-Kobe study (2008-2015) on anomalous heat effects (AHE) by interaction of nano-metals and D(H)-gas is presented in three parts.

Part-I) D(H) isotopic effect by twin gas loading and calorimetry at room temperature is reviewed.

Part-II) AHE by interaction of binary Ni-based nano-metals and H(D)-gas at 200-300 deg C is reviewed.

Part-III) Theoretical explanation by advanced TSC-models is briefly reviewed.

AHE at room temperature was significant only in dynamic evolution of D-absorption, cf. H-absorption, and considerable D(H)-isotopic effect for integrated heat values. AHE lasting for several days has been observed at elevated temperatures in the range of 200-300 deg C. AHE has been confirmed by repeated observation of excess heat-power. AHE was lasting for long time span as several days for CNS, PNZ and CNZ samples. AHE has been seen after D(H) loading ratios saturated. AHE is therefore some catalytic surface sited effect by in/out of D(H)-gas. Observed long lasting heat gave order of GJ/mol-H(D) (or several keV/atom-H(D)) in a few days span. Level is not of H(D) chemical absorption energy, so far. AHE at 200-300 deg C is almost impossible to explain by known chemical reactions. Pd-only nano-metals did not work at higher temperatures than 100 deg C. AHE were observed both for H- and D-charging at 200-300 deg C.

Keywords: Nano-metals, anomalous heat effect, Pd, Pd-Ni, Cu-Ni, Nano-composites, H and D-gas charge, room temperature, elevated temperature, sustainable heat, 1 keV/H(or D), D(H)-cluster, nano-catalyst, TSC theory, 4D-fusion, 4H WS fusion.

1. Introduction

Akito Takahashi has studied so called cold-fusion or condensed matter nuclear reactions (CMNR) since 1989 after the famous Fleischman-Pons claim, as seen in many papers compiled in ISCMNS Library [1]. He with his team at Osaka University has seriously done the heavy water Pd-cathode experiments to search correlation between excess power and nuclear signatures like neutrons, gamma-rays, X-rays and He. They have however suffered with the problem of very difficult reproducibility. They have also studied on if anomalies appeared in the interaction of low-energy-beam and metal-deuterium targets, and have observed repeatedly the huge enhancement of d-d-d three-body fusion events [3]. A. Takahashi has developed a series of theoretical models on multi-body fusion in metal-

deuterium system as reviewed its early stage development in [4]. A. Takahashi retired from Osaka University in 2004 and started to work at Technova Inc. for further R&D of CMNR. Technova has planned a new program in 2007 to implement nano-metal D(H)-gas loading experiments, intrigued by Arata-Zhang work [5]. Background for the Technova new program is explained in [6] which was not accepted for publication by journals and magazines, by unknown reasons. However, Technova team concluded that the D(H)-gas loading method should be employed for R&D since the reproducibility problem would be easier to clear by pureness and cleanness of nano-metal samples in gas phase interactions and we would be able to get rational insights on underlying physical mechanisms. And the team thought that the feasibility to realize energy producing industrial devices by CMNR would be more promising in the gas-phase reaction at elevated temperatures of running energy convertor to electricity power. The team looked for a collaborator to implement gas-phase experiments and got agreement with Akira Kitamura, Kobe University, who joined CMNR studies in 1990s to have published works with low-energy d-beam experiments [2]. Later Kitamura joined the Technova Inc. after his retirement from Kobe University. Thus the Technova-Kobe U collaboration has started in 2007 and constructed the twin D(H) gas loading experiment system with water mass-flow calorimetry in 2008. Using nano-Pd based powder samples, a systematic study has been done in 2008-2012 for studying isotopic effects between D-gas and H-gas loading in gas absorption rates (dynamic D(H)/Pd loading ratios) and heat-power evolution data, as we review in Section-2 (Part-I). In 2013-2015, the experimental system was revised with 10 times larger reaction chamber under oil-mass-flow calorimetry which enabled to carry out scaled up heat-power runs at elevated temperatures up to 300 deg C oil-outlet temperature. Results by the revised system are reviewed in section 3 (Part-II). A. Takahashi, et al has extended the cluster fusion model in parallel works, and the so called Takahashi TSC theory is now becoming a series of established system of various sub-models, as major published papers are compiled in [7] (preprints are downloadable there). Brief review of explanation of CMNR by the TSC theory is given in Section 4 (Part-III).

2. Part-I D(H) Isotopic Effects in Nano-Pd Twin Gas Loading Experiments

The Arata-Zhang work initiated the use of powder of Pd-nano-metals supported in zirconia [5] to report impressive power-temperature evolution from the start of D-gas charging. They reported clear data of He-4 generation only for D-gas charging (no He-4 generation for H-gas charging). As their calorimetry method was of rather primitive way by cell temperature comparison with the blank H-charging runs, Technova-Kobe team employed a sophisticated water-mass-flow calorimetry system with dynamic (time-dependent) measurements of heat-power evolution and D(H)-loading rates in nano-metal samples, by the twin system as shown in Fig.1, so as to improve accuracy of calorimetry and to obtain dynamic physical quantity of D(H) sorption energy. A systematic view of one of twin cells is illustrated in Fig.2. To realize a high precision of calorimetry, room temperature of the facility cabin was regulated with 25 ± 0.1 deg C by a spindle air-conditioner, and coolant water inlet-temperature was controlled with 25 ± 0.1 deg C by constant-temperature water bath. The calorimetry system was observed to be stable for long runs as for several weeks.

The basic physical idea for test nano-metal powder samples is explained by Fig.3. From our theoretical insight [7], nano-metal particle will work as mesoscopic catalyst on its surface non-uniform sub-nanometer scale structure. Optimum size of nano-metal particle will be in the range of 2-20 nm, namely the mesoscopic size. It was considered that nano-metal particles are better to separate from each other to prevent the formation of larger particle by hydrogen charging and temperature elevation, since we know that larger Pd particle than 100 nm diameter worked

as bulk Pd H-absorption performance [8]. TEM image of used nano-Pd/meso-silica powder is shown in Fig.4. Existence of larger Pd particles (eg. 100nm size) weakens the AHE observation.

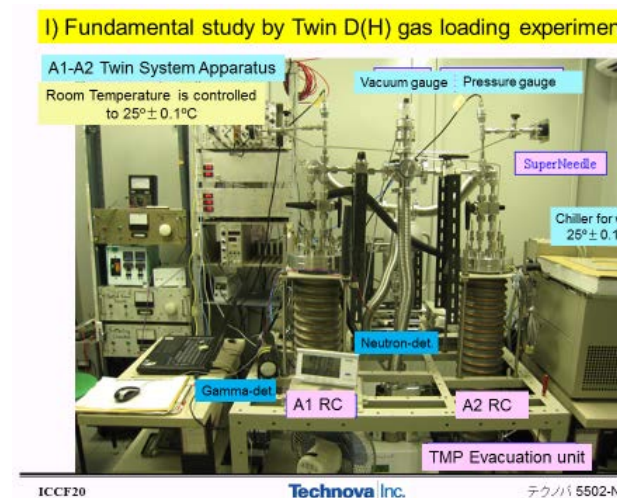


Fig.1 The Technova-Kobe twin system for D(H)-gas loading

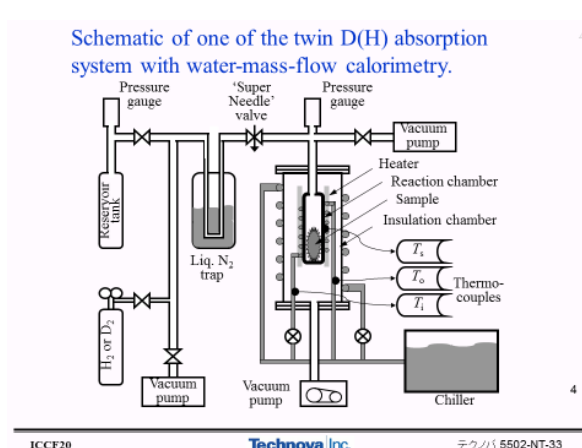


Fig.2 Schematic diagram of one of twin cell

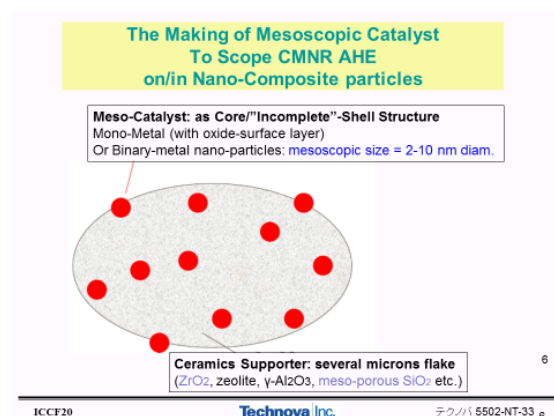


Fig.3 Design idea of nano-metals supported by ceramics

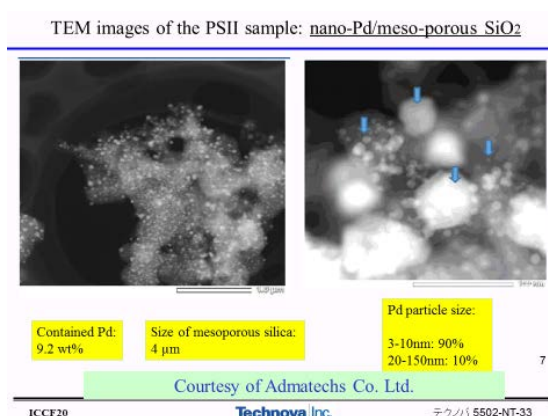


Fig.4 TEM image of nano-Pd supported by meso-silica flake

We have tested various nano-Pd based powders, Pd-Ni binary nano-particle powders and Cu-Ni binary nano-particle powders as listed in Table-1 [8-11]. Results of anomalous D/H isotopic effect observed by the twin system in 2008-20012 are summarized in Table-2 [8-11]. Most interesting results are by Pd₁Ni₆/zirconia sample (PNZ2B). This sample was produced by the melt-spinning and oxidation technique and similar samples will be shown in Section 3 (Part-II). Comparing PNZ and PNZ2B in Table-2, we see smaller content of Pd in Pd-Ni binary nano-particle gave more enhanced heat-power bursts. What is the reason? We speculate that catalytic potential on nano-particle surface may be much deeper at sub-nano-hole made by the incomplete shell structure of Pd-atoms on Ni-

core [10]. The TSC formation in sub-nano-hole (SNH) may induce 4D fusion and 4H-WS fusion, as we explain in Part-III [see also Ref. 10]. Nano-Ni/zirconia powder sample did not show any measurable D(H)-absorption and heat power evolution at room temperature (around 25 deg C). However, by using binary Pd-Ni nano-particle supported by either meso-silica or zirconia we observed significant D(H)-absorption and heat bursts at room temperature runs. Especially heat bursts by Pd₁Ni₇/zirconia at room temperature was observed largest.

Samples tested for Part I study ICCF20

	Pd / (Cu)	Ni	Zr	Si	O	Supplier	
100nmφ-Pd PP	99.5%, 100nmφ	---	---	---		Nilaco Corp.	[1],[2]
Pd-black PB	99.9%, 300mesh	---	---	---		Nilaco Corp.	[1],[2]
mixed oxide PZ	0.312 (8nmφ)	---	0.688	---	(1.69)	Santoku Corp.	[1],[2],[3]
mixed oxide PS	0.054 (2-10nmφ)	---	---	0.946	(1.95)	Admatechs Corp.	[5]
mixed oxide NZ	---	0.467	0.533	---	(1.53)	Santoku Corp.	[2]
mixed oxide PNZ / PNZII	0.080 / 0.023	0.352 / 0.891	0.568 / 0.292	---	(1.57) / (1.50)	Santoku Corp.	[2]
mixed oxide PNZ2B	0.04	0.29	0.67	---	(1.67)	Dr. B. Ahern	[4]
mixed oxide CNZI	(Cu) 0.08	0.35	0.57	---		Santoku Corp.	[6]

Technova Inc. テクノバ 5502-NT-33

Tested Metal/Ceramics Powders and Summary Results by Part-I Study ICCF20

	Pd	Ni	Zr	O	Supplier	Anomalies observed?
100nmφ-Pd PP	99.5%, 100nmφ	---	---	---	Nilaco Corp.	[1],[2] No, bulk metal data
Pd-black PB	99.9%, 300mesh	---	---	---	Nilaco Corp.	[1],[2] Yes, a little large heat & D/Pd
mixed oxide PZ	0.346	---	0.654	(1.64)	Santoku Corp.	[1],[2],[3], discussed Yes, Heat and D/Pd reproducible
mixed oxide NZ	---	0.358	0.642	(1.64)	Santoku Corp.	[2] No heat and loading
mixed oxide PNZ	0.105	0.253	0.642	(1.64)	Santoku Corp.	[2] Yes, but weak
mixed oxide PNZ2B	0.04	0.29	0.67	(1.67)	Dr. B. Ahern	Yes, very large heat and D(H)/M, reproducible

Technova Inc. テクノバ 5502-NT-33

Table-1: Sample powders tested in Part-I study [10]

Table-2 Summary results of Part-I study

Only a few examples of obtained data are shown in the following figures. Fig.5 shows the first significant results we obtained in 2008[8]. The smaller was the Pd particle, the more enhanced heat burst was observed.

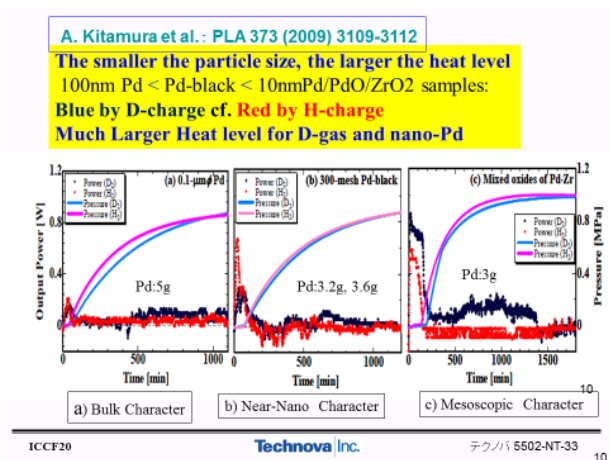


Fig.5 First significant data by the twin system

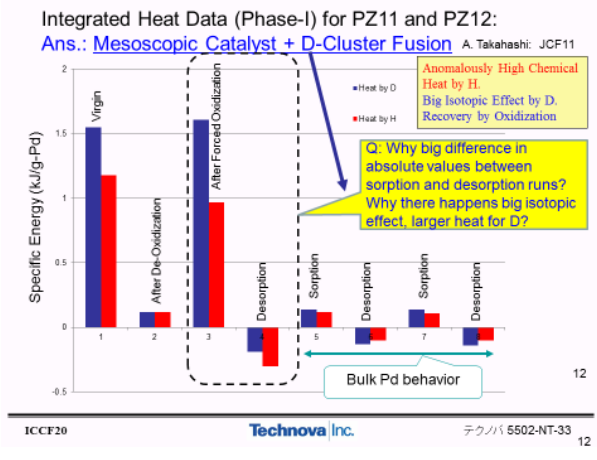


Fig.6 Integrated heat burst-data by nano-Pd/zirconia

Fig.6 shows time-integrated heat burst data by nano-Pd/zirconia powder samples. Forced oxidation reactivated the enhanced heat bursts, and D-gas loading gave significantly larger heat level (blue) although D/Pd and H/Pd loading ratios were almost the same values. PdO surface layer of nano-Pd particle may have a role to generate catalytic sub-nano-hole (SNH) when D(H)-gas was initially introduced into the reactor cell, as discussed detail in [12].

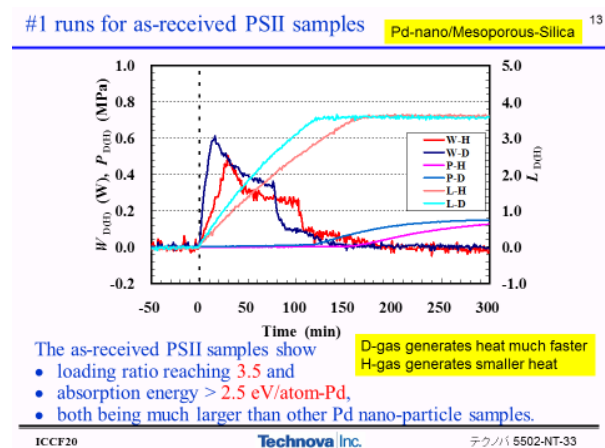


Fig.7 typical D(H)-loading and heat burst data by Pd(8nm)/meso-silica

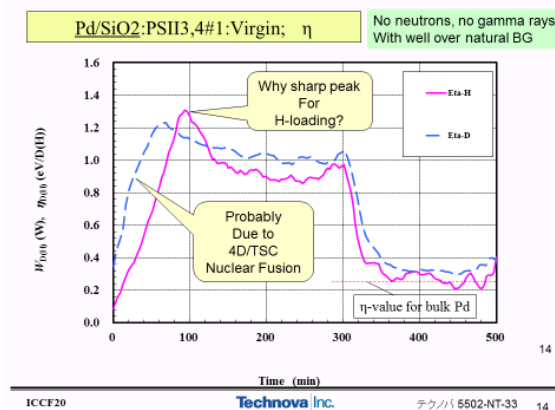


Fig.8 Dynamic sorption energy data (η values) for similar data shown in Fig.7

Pd-nano-particles supported in mesoporous silica worked in similar way as Pd/zirconia samples. Example of data are shown Fig.7 and Fig.8. D/Pd and H/Pd loading ratios became very large as 3.5 even under the very low pressure as near vacuum, although we know 0.7 is the limit of loading ratio of bulk Pd material under high D(H)-pressure such as 100 MPa. Dynamic sorption energy is very large as 1.0-1.2 eV/D(H) in the early time zone and dropped to smaller values as 0.22 eV that is thought to be absorption energy of D or H in bulk Pd sample. We have considered the tail of ca. 0.22 eV was correspondent to D(H)-absorption by large Pd particles existed in the used powder sample (see Fig.4). No neutron and gamma-ray counts exceeded natural BG were observed.

Using the twin system without water coolant, AHE measurements have been conducted at elevated temperatures in 100-400 deg C [13]. Interestingly, Cu₁Ni₇/zirconia and Cu₁Ni₇/mesosilica samples with H-gas charging have given excess heat evolution for several weeks long run, almost continuously (sustainable AHE), and D-gas charged runs did not show much AHE as the H-gas charging gave. We have been intrigued to confirm this interesting results which may give good hints toward industrial application, because of sustainable heat evolution at higher temperatures as 200-400 deg C. The Part-II stage study was initiated so far.

3. Part-II AHE by interaction of binary Ni-based nano-metals and H(D)-gas

Figure 9 shows schematic diagram of revised oil-mass-flow calorimetry system with enlarged (500 cc) reaction chamber. The first result with the system was reported at ICCF18[14] and advanced experiments at ICCF19 [15].

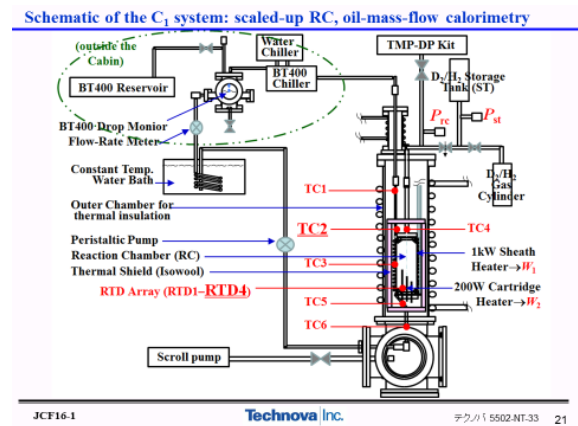


Fig.9 The advanced Technova-Kobe oil-mass-flow-calorimetry system for elevated temperature D(H)-gas charging study[14, 15, 17]

Parameters of the PNZt sample and chamber volumes

	At. %/Weight	Weight fraction	Mass (g)	Dens. (g/cc)	Vol. (cc)	Num. of Moles	Molar fraction
PNZt			28.660				
2015.713	O	0.24376	9.421			5.889E-01	0.650182
	Ni	0.16570	6.415	8.908	0.720	1.093E-01	0.3058174
	Pd	0.04376	1.662	8.940	0.186	1.561E-02	0.0439444
charged	Zr	0.54746	21.182	5.700	3.713	2.320E-01	0.650182
	ZrO2	123.222	1334.560	5.700	234.133	1.083E-01	

Reaction Chamber	Inner D. (cm)	Length (cm)	Capacity (cc)	Cumul. Total
Body	5.6	15.5	381.766	
Transition cone	5.6	2.65	24.790	
	4.1	1.9	8.362	
Ends	4.1	1.5	39.608	448.164
heater	1.46	-6	-10.045	
heater/Flange	3.4	0.85	7.717	
3/8"-1" tube	0.753	47.2	21.019	
1/2" tube	1.02	43	35.137	501.992
sample			-738.752	
Source Tank			763.240	-Vrc
Body	6.93	2.44	920.326	
ICF70-a	3.5	0.5	4.811	
ICF70-b	4	1.27	15.959	941.105
1/4"-12" tube	0.385	330	38.417	
			979.523	-Vat

Table-3 Sample setting conditions for the oil-mass-flow calorimetry experiment [17]

Pd and Ni are present in the same region as a whole, having mesoscopic structure.

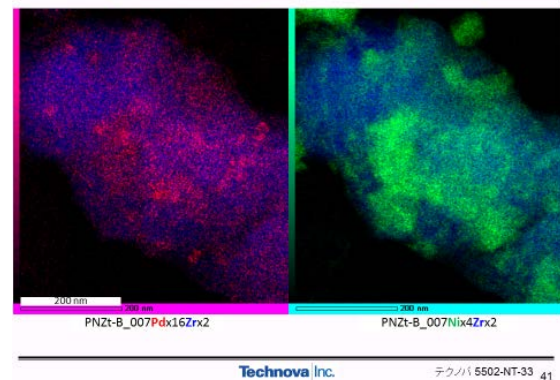


Fig.10 STEM/EDS image of Pd₁Ni₇/zirconia sample before D-gas charging [17]

Particle distribution not changed by the absorption runs: After Run

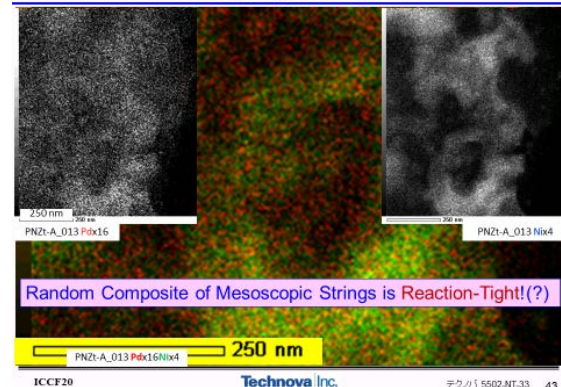


Fig.11 STEM/EDS image of Pd₁Ni₇/zirconia sample after D-charging runs [17]

Table 3 shows typical setting conditions with PNZ(Pd₁Ni₇/zirconia) sample. PNZt and CNZt samples were fabricated by the melt-spinning method [17] at Turin University, Italy and oxidized at Kobe University. The STEM/EDS images of PNZt sample before and after the D-absorption runs are shown in Fig. 10 and Fig.11. Comparing with Pd/meso-silica sample in Fig.4, nano-structure of melt-spinning (glass-metal) and oxidation (nano-particle formation) PNZt sample is complicated. The EDS image shows Pd-atoms and Ni-atoms are locating in same positions with complex mesoscopic structure like twisted assembly of meso-strings. We have found PNZ and CNZ type melt-spinning/oxidation samples have shown repeatable D- or H-absorption performance with high D(H)/M(binary-metal) loading values, and sustainable AHE at elevated temperatures (200-300 deg C), after D(H)/M loading ratios were saturated. The complex mesoscopic structure like twisted assembly of meso-strings

can be background of damage-tight structure for AHE generation, which may be due to the CMNR consequence, namely nuclear heating. AHE data for PNZt at elevated temperatures are shown in Fig.12 and Fig.13 [17].

AHE Power = W_{ex} and Loading Ratio L_M (=D/Pd-Ni or H/Pd-Ni)

As the PNZt sample took only 4 % of RC volume, we expect significant increment of Excess Power level if we realize 100% filling of the sample in RC!

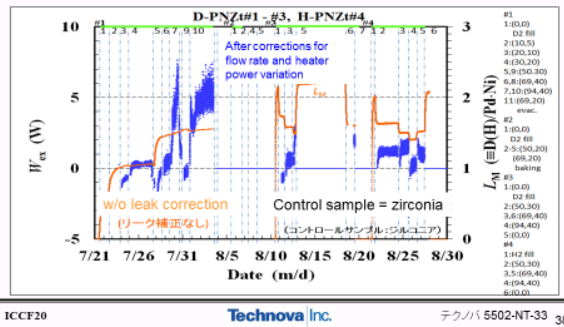


Fig.12 evolution of excess power data (blue) for PNZt sample in 200-300 deg C cell temperature condition

Integrated AHE E_{ex} and η_{av} (heat per D(H)-transfer) for PNZt 200-300° C

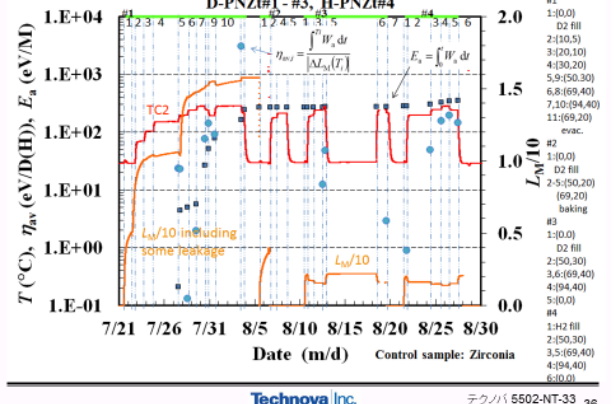


Fig.13 Relation among D/M loading ratio (orange), oil-outlet temperatures (red), η -values (blue dots) integrated heat energy E_a (black square)

Excess Power W_{ex} and Loading Ratio L_M (=D/Ni or H/Ni): for higher T

As the CNZt sample took only 4 % of RC volume, we expect significant increment of Excess Power level if we realize 100% filling of the sample in RC!

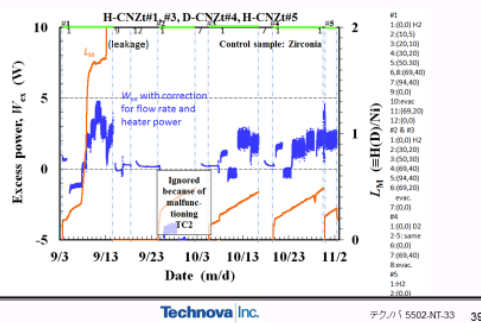


Fig.14 Excess power evolution data (blue) for Cu1Ni7/zirconia sample, compared with H/M(Ni) loading ratios

Excess Energy E_{ex} and Phase-averaged η_{av} (heat energy per H-movement)

AHE: 6-8 keV/atom-H = 0.6 to 0.8 GJ/mol-H must be non-chemical origin. AHE happened in the condition of post saturated H-loading.

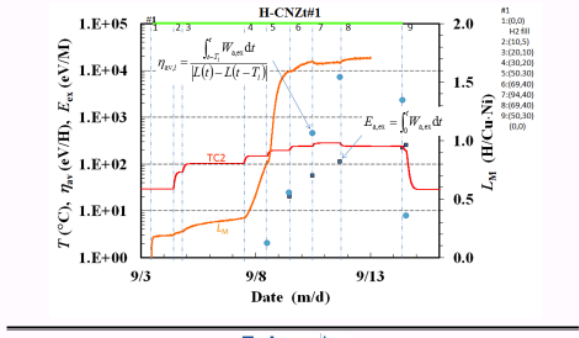


Fig.15 AHE data for Cu1Ni7/zirconia sample, comparing H/Ni loading ratios (orange), oil-outlet temperatures (red), η -values (blue dots) and integrated heat data E_a (black squares)

Excess power of ca. 5 W at around 300 deg C cell temperature continued for about one week, after D/M loading ratios were saturated. If we consider that the excess heat was caused by deuterium-metal interaction, change of D/M data, during the phase of every supplied external heater power as inserted right end of figures as [W1, W2] two heater input powers (see Fig.9), should be taken as transferred D-atoms by the AHE reactions, with which data are given as η -

values (blue dots) in Fig.13. The obtained η -values (blue dots) exceeded 1 keV/D-atom (100 MeV/mol-D) level, which is impossibly difficult to explain by known chemical reaction energies for hydrogen interactions [18].

Similar data with H-gas charging for Cu₁Ni₇/zirconia sample by melt-spinning/oxidation are shown in Fig.14 and 15. Observed AHE data for CNZ type samples with H-gas charging should be a mystery in the common view of nuclear reaction theories. The view of the first author (A. T.) is of effect by a new type of condensed matter mediated reaction, by 4H/TSC end-state oscillation to cause 4H WS fusion as explained in the Theory Section (Part-III). In the view of industrial application, the AHE data by CNZ with H-gas is most intriguing because of cheap abundant materials for making energy-generation devices with its higher temperature heat generation property.

We have also obtained similar AHE data for Cu₁Ni₇/meso-silica powder samples [15]. Comparison of heat generation and D(H)-absorption data between PNZ, PNS, CNZ and CNS type samples are given in Table-4 and Table-5.

Summary II: Comparison of melt-spinning and mp-silica supported

	M	PNZt	PNSII/Al ₂ O ₃
Transient phase at RT in #1 run	Loading ratio (H/M)	9.0±1.0 (1.1)	3.2 (0.58)
	Specific power (W/g-M)	1.3 (0.26)	3.9 (0.80)
	Sorption energy (eV/atom-M)	16±2.0 (2.0)	3.0 (0.55)
Transient phase at RT in #2 or later	Loading ratio (H/M)	13±1.0 (1.6)	0.94±0.06 (0.17)
	Specific power (W/g-M)	1.1±0.3 (0.22)	0.39±0.04 (0.080)
	Sorption energy (eV/atom-M)	6.1±0.7 (0.7)	0.20±0.01 (0.036)
Saturation phase at elevated temp.	Max. excess power (W)	12±2	10±1
	Max. specific excess power $W_{s,ex}$ (W/g-M)	7.2±1.2 (1.5)	6.4±0.5 (1.2)
	Specific excess energy $E_{s,ex}$ (keV/atom-M)	0.6 (0.08)	3.8 (0.68)
	Phase-averaged sorption energy η_{av} (keV/atom-H)	0.8 ~ 7.0	2.2 ~ 6.5

* 'Loading' in #1 runs might include hydrogen atoms spent for deoxidation of PdO or NiO.
** 'H' stands for either H or D, and 'M' stands for either Ni or Pd.

ICCF20

Technova Inc.

テクノバ | 5502-NT-33 46

Summary II: Comparison of melt-spinning and mp-silica-supported

	M	CNZt	CNS2
Transient phase at RT in #1 run	Loading ratio (H/M)	Ni	Ni
	Specific power (W/g-M)	0.17±0.02	~0
	Sorption energy (eV/atom-M)	(2.2±0.2)E-1	~0
Transient phase at RT in #2 or later	Loading ratio (H/M)	0.17±0.02	---
	Specific power (W/g-M)	(2.7±0.3)E-2	---
	Sorption energy (eV/atom-M)	(3.4±0.3)E-2	---
Saturation phase at elevated temp.	Loading ratio (H/M) in #1 run	0.17±0.02	0.9
	Loading ratio (H/M) in #2 or #3	0.15±0.02	0.12 - 0.08
	Max. excess power (W)	12±2	10
	Max. specific excess power $W_{s,ex}$ (W/g-M)	1.3±0.2	0.8
	Specific excess energy $E_{s,ex}$ (keV/atom-M)	0.26±0.03	0.38
	Phase-averaged sorption energy η_{av} (keV/atom-H)	0.45 ~ 6.0	15

* 'Loading' in #1 runs might include hydrogen atoms spent for deoxidation of PdO or NiO.
** 'H' stands for either H or D, and 'M' stands for either Ni or Cu.

ICCF20

Technova Inc.

テクノバ | 5502-NT-33 47

Table-4 Comparison of AHE data for PNZ and PNS type samples

Table-5 Comparison of AHE data between CNZ and CNS type samples

We summarize the obtained knowledge as follows.

- 1) AHE has been observed at elevated temperatures in 200-300 deg C.
- 2) AHE has been confirmed by repeated observation of excess heat-power.
- 3) AHE was lasting for long time span as several days.
- 4) AHE has been seen after D(H) loading ratios saturated.
- 5) AHE is therefore some surface sited effect by in/out of D(H)-gas.
- 6) Observed long lasting heat gave several GJ/mol-H (or several tens keV/atom-H).
- 7) Level is not of H(D) absorption energy.
- 8) AHE at 200-300 deg C is impossible to explain by chemical reactions.
- 9) Pd only nano-metals do not work at higher temperatures than 100 deg C.
- 10) Pure-Ni-nano-metal powder did not work well at room and elevated temperatures.

4. Part-III Theoretical Explanation by TSC-based Models

In the recent short review paper [19], A. Takahashi wrote: The basic concept is that the ordering/constraint conditions of particles (namely deuterons, protons and electrons) in condensed matter containing deuterium (D) and/or protium

(H) should make unique ‘hitherto-unknown’ multi-body D(H)-cluster fusion reactions measurable under the dynamic constraint ordering condition of surface/solid state-physics of D(H) + condensed matter, while the known fusion reactions in high temperature plasma are always two-body reactions as p-d, d-d, d-t, d-³He and so on, which are taking place in random free particle motions. Here, D(H)-cluster includes two deuterons (or protons) systems as d-e-d (p-e-p) and d-e-e-d (p-e-e-p), as well as 3D(H), 4D(H), 6D(H) and so forth. And e denotes electron. Here D denotes deuteron (d) + electron (e), and H does p + e too. In the conventional nuclear physics view, the two body collision process is predominant mechanism for nuclear fusion and the multi-body nuclear interaction events are negligible. However, the author has found by the QM-Langevin code analysis that Platonic symmetry D-clusters could make very rapid (1-5fs) condensation motion to reach ‘collapse’ getting into nuclear strong interaction range (several fm) with very enhanced Coulomb barrier penetration probability and could induce almost 100% 4D fusion per TSC formation for the case of a 4D-cluster. Similar collapsed condensation would happen for 6D and 8D systems too. The theory was extended for light hydrogen (proton) system. He has also found that 2 D(H) systems as d-e-d three body confinement cannot make enhanced barrier penetration even at the minimum d-d (or p-p) approaching distance happening for a short time moment of dynamic motion. Only larger Platonic clusters than 3D(H) can have the collapsing one - through condensation. The prediction of final nuclear products (ash) was done based on the nucleon-halo model for intermediate compound states, like ⁸Be* by the 4D/TSC-fusion and ⁴Li* by the 4H/TSC WS (weak-strong rapid cascade) fusion. Especially, the proposed excitation energy damping model of BOLEP (burst-of-low-energy-photons) via nucleon-halo state rotation/vibration modes is thought to be the mechanism for producing, free of hard radiation, a helium ash product with excess heat evolution in metal-deuterium systems. Predicted discrete peaks of minor alpha-emission agreed quite well with the Russian experiments.

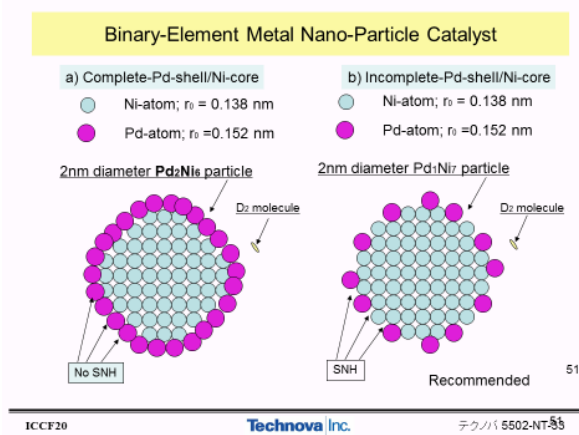


Fig. 16 Model of binary nano-metal catalyst

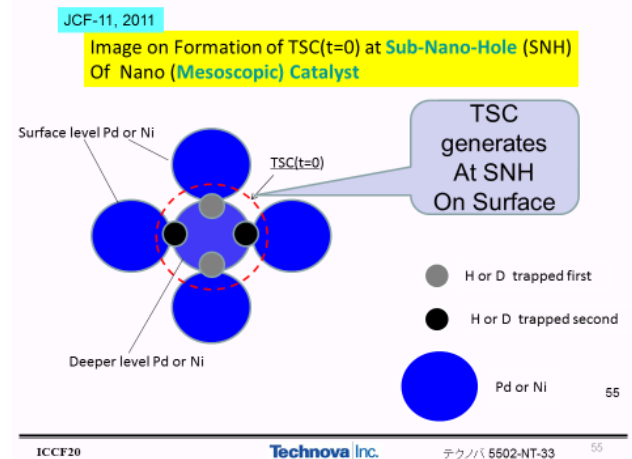


Fig.17 Model of TSC formation site on surface of nano-catalyst

More extended review papers are in [20-22]. A general introductory review on cluster fusion theory is given in [23]. Preprints of [20-23] are downloadable at [7].

Most interesting results of similar calculations based on the QM-Langevin equation [24, 25] are of collapsing condensation (one way to collapse), happened for larger clusters as 4D(or H)/TSC, 6D(or H)/RDC and 8D(or H)/RDC [23], and 2D(or H) and 3D(or H) systems got to stable ground states with inter-nuclear distances of ca. 100pm. Therefore, we have no chance to make “cold fusion” by 2D(or H) and 3D(or H) systems in condensed matter. Models of 4D(or H)/TSC formation site with nano-metal particle surface are shown in Fig.16 and Fig.17 [10, 19, 20, 23]. Formation of sub-nano-holes (SNH) on surface of binary metal particles of incomplete-shell/core type (Fig.16) may have essential role to make a global mesoscopic potential [10] which has deep adsorption well for trapping D₂ (or H₂) molecule of gas-phase. By trapping at a SNH site, D₂ (or H₂) will lose freedom of rotation. Before the dissociation of trapped D₂ (or H₂) molecule at the SNH site, another D₂ (or H₂) molecule may come in the site to make orthogonal (90 deg rotated state of two molecules) coupling to form TSC(t=0) state. Once a 4D(or H)/TSC is formed, it makes a

very rapid condensation motion as simulated by the QM-Langevin equation with HMEQPET pseudo potentials [22-26]. The latest simulation paper for 4H/TSC [26] reports an interesting feature of chaotic end-state oscillation as shown in Fig. 18.

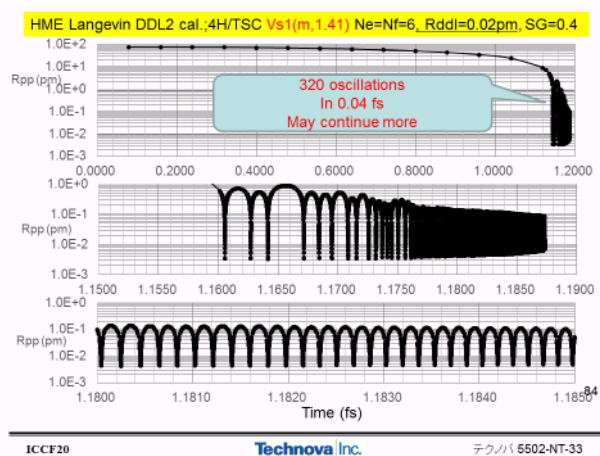


Fig.18 Simulation of 4H/TSC condensation motion by HME-Langevin code [26]

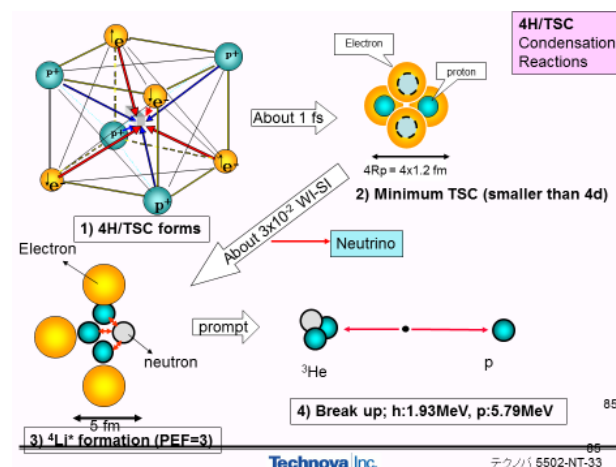


Fig.19 Illustration of 4H/TSC condensation and WS fusion

4H/TSC gets into the end-state (there is a limiting p-p distance of 2.4 fm between protons due to hard core of proton-nucleon (uud quark-state)) in 1.16 fs. The simulation of Fig.18 is done by taking relativistic motion of electrons. 320 times chaotic oscillations are drawn at the end state (calculation stopped there by the used PC memory limit), and we speculate the chaotic oscillation within 100-4.0 fm p-p distance will continue more. If the chaotic end state oscillations continue more than 1.0 fs, 4H/TSC-end-state will induce ca. 3% of WS fusion (WI weak-interaction to SI strong interaction happens almost simultaneously) per a 4H/TSC formation. Ca. 200 W/mol-Ni WS fusion heat power may happen [26] by this process, which can be an explanation of AHE by PNZ and CNZ samples with H-gas charge. Figure 19 illustrates the feature of 4H/TSC condensation motion and WS fusion in 4 steps.

4D/TSC condensation will get to the d-d distance of 20 fm in 1.4 fs [25], and 4D-simultaneous fusion happens 100% before the 20 fm d-d distance state came, and therefore the 4D/TSC end-state has no chaotic oscillations as seen for 4H/TSC end state. We copy the feature of 4D/TSC condensation motion and 4D-fusion products in Fig.20. In the PNZ or CNZ experiments, we have observed ca. 5 W heat-power level with ca. 0.1 mol Ni-based nanoparticles. A 2 nm diameter Ni particle contains ca. 1000 Ni atoms. 0.1 mol Ni has $6.23E+22$ Ni atoms. Namely ca. $6.23E+19$ Ni nanoparticles were used in the PNZt experiment. 4D/TSC formation rate of 10^{11} tsc/s generates heat power of 1.0 W. 5 W level power can be generated by 4D/TSC formation rate of 1.0 tsc/s per $1.0E8$ Ni-based nanoparticles, namely $1.0E-8$ tsc/s/nano-particle. This looks feasible rate for explanation of observed AHE heat-power level by D-gas-charging.

Finally, we copy the summary of theoretical predictions by TSC models [21] in Fig.21. Now most of key experimental claims on AHE and CMNR can be explained by the TSC cluster fusion theory as for CMNR mechanisms, although no reports on nuclear ash by H-gas interaction with nano-metals have been provided by researchers at this stage.

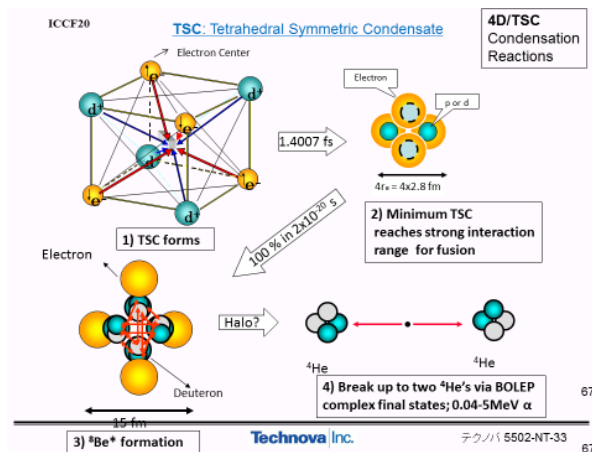


Fig.20: Illustration of 4 steps in 4D/TSC condensation and 4D fusion process

Why so radiation-less results?

	Claims by Experiments	Predictions by TSC Models
MDE (Metal Deuterium Energy)	Heat: $24 \pm 1 \text{ MeV}/^4\text{He}$ (Miles, McKubre, et al) Weak alpha-peaks (Lipson, Roussetskii, etc.) Weak neutrons (Takahashi, Boss, etc.) X-rays burst (Karabut, et al.)	$23.8 \text{ MeV}/^4\text{He}$ by 4D/TSC fusion with low-E alphas (46keV) Minor alpha-peaks by nucleon-halo BOLEP minor decay channels High-E neutron by minor triton emission BOLEP in ca. 1.5keV
MHE (Metal Hydrogen Energy)	Heat w/o n and gamma unknown ash (Piantelli, Takahashi-Kitamura, Celani, etc.)	4H/TSC WS fusion $7.2 \text{ MeV}/^3\text{He}$ and d Very weak secondary Gamma and n Ca. 10^{-11} of ^3He and d

Fig.21 Slide summary of predictions by the TSC theory

5. Concluding Remarks

From the 8 years (2008-2015) collaboration study of Technova-Kobe team, the following concluding remarks can be stated.

The anomalous heat effect (AHE) exists in the interaction of nano-metals and hydrogen gas. Two kinds of AHE phenomena have been observed. One is the burst-like AHE during the dynamic evolution of D(or H)-absorption which started strongly from the beginning of D(H)-gas charging to powder samples of Pd or binary Pd-Ni nano-particles supported in ceramics flakes, at room temperature. The other is the sustainable (long time lasting) AHE after the saturation of D(H)-loading ratios, at elevated temperatures (200-300 deg C). Reproducibility is very well.

The burst-like AHE has significant D(H)-isotopic effect in the beginning phase of D(H)-absorption. No isotopic differences have been found between D-loading and H-loading ratios, although D(H)/M loading ratios were observed to be larger than 3.0 (namely much larger than 0.7 for bulk Pd-metal). Big isotopic differences were observed in dynamic (time-dependent) sorption energy (η -value); η -values for D-charging exceeded 1.0 eV/D-sorption and appeared much faster than those for H-charging. This phenomenon seems a new process in CMNS and is difficult to explain by known chemical (electron-exchange bonding) processes. However, η -values for H-charging exceeded 1.0 eV/H-sorption has happened with significantly large time lag after those by D-charging. Time averaged η -values for D-charging were several tens % larger than those for H-charging. Since H-charging induced AHE as well as D-charging, more than half of AHE burst at room temperature is thought to be caused by the enhanced adsorption potential (global mesoscopic potential) of nano-metal particles. However, the faster and larger AHE burst by D-charging is speculated to be by some nuclear reactions like the 4D/TSC fusion to produce ^4He ash without radiations.

The sustainable AHE as observed for Pd₁Ni₇/zirconia (or /meso-silica) and Cu₁Ni₇/zirconia (or meso-silica) at elevated temperatures (200-300 deg C) have been repeatedly observed after D(H)/M dynamic loading ratios saturated. Averaged η -values at the elevated temperature conditions exceeded 1 keV/D(H) (or 100 MJ/mol-D(H)-transferred). So the explanation by chemical reaction origin is very difficult to fit to this observation. We have given the explanation by the condensed cluster fusion theory (TSC models) as 4D/TSC fusion for D-charging and 4H/TSC WS fusion for H-charging. Why AHE by H-charging showed comparable (or more) excess heat-power to those by D-charging is of mystery to be studied further. However, the sustainable AHE power by Cu₁Ni₇/zirconia with H-gas charging is very promising result to look forward its industrial application of cheap distributable thermal energy devices.

References

- [1] ISCMNS Library, <http://www.iscmns.org/library.htm> , see papers by Akito Takahashi
- [2] *ibid.*, see papers by Akira Kitamura
- [3] A. Takahashi, K. Maruta, K. Ochiai and H. Miyamaru, Phys. Lett. A, 255, 89-97, 1999
- [4] Akito Takahashi, J. Condensed Matt. Nucl. Sci., Vol.4, 269-281, 2011
- [5] Y. Arata and Y. Zhang, J. High Temp. Soc., Special Issue, Vol1, 2008
- [6] Akito Takahashi, <http://vixra.org/pdf/1502.0207v1.pdf>
- [7] http://vixra.org/author/akito_takahashi see 15 pdf pre-print-papers
- [8] A. Kitamura, T. Nohmi, Y. Sasaki, A. Taniike, A. Takahashi, R. Seto and Y. Fujita, Phys. Lett. A, 373, 3109-3112, 2009
- [9] A. Kitamura, Y. Miyoshi, H. Sakoh, A. Taniike, Y. Furuyama, A. Takahashi, R. Seto, and Y. Fujita, T. Murota and T. Tahara, J. Condensed Matt. Nucl. Sci., Vol.13, 277-289, 2014
- [10] A. Takahashi, A. Kitamura, Y. Miyoshi, H. Sakoh, A. Taniike, R. Seto and Y. Fujita, Proc. JCF-11, 47-52, 2011
- [11] H. Sakoh, A. Kitamura, Y. Miyoshi, A. Taniike, A. Takahashi, R. Seto and Y. Fujita, *ibid.*, pp.16-22
- [12] A. Takahashi, R. Seto, Y. Fujita, A. Kitamura, Y. Miyoshi, H. Sakoh and A. Taniike, J. Condensed Matt. Nucl. Sci., Vol.5, 17-33, 2010
- [13] A. Takahashi, A. Kitamura, R. Seto, Y. Fujita, A. Taniike, Y. Furuyama, T. Murota and T. Tahara, J. Condensed Matt. Nucl. Sci., Vol.15, 23-33, 2015
- [14] A. Kitamura, A. Takahashi, R. Seto, Y. Fujita, A. Taniike, Y. Furuyama, J. Condensed Matt. Nucl. Sci., Vol.15, 231-239, 2015
- [15] A. Kitamura, A. Takahashi, R. Seto, Y. Fujita, A. Taniike, Y. Furuyama, J. Condensed Matt. Nucl. Sci., Vol. 19, 135-144, 2016
- [16] S. Yamaura, H. Kimura and A. Inoue, Materials Transactions, Vol.44, 696-699, 2003
- [17] A. Kitamura, E. Marano, A. Takahashi, R. Seto, T. Yokose, A. Taniike and Y. Furuyama, Proc. JCF-16, pp. 1-16, 2016
- [18] A. Kitamura, A. Takahashi, R. Seto, Y. Fujita, A. Taniike and Y. Furuyama, Current Science, Vol.108, 589-593, 2015
- [19] Akito Takahashi, Current Science, Vol.108, 514-515, 2015
- [20] Akito Takahashi, J. Physical Science and Application, Vol.3, 191-198, 2013
- [21] Akito Takahashi, J. Condensed Matt. Nucl. Sci., Vol.15, 11-25, 2015
- [22] Akito Takahashi, J. Condensed Matt. Nucl. Sci., Vol.19, 298-315, 2016
- [23] Akito Takahashi, Proc. JCF-15, 63-90, 2015
- [24] A. Takahashi, American Chemical Society, LENRSB (Low Energy Nuclear Reaction Source Book) 2 (2009) 193-217
- [25] Akito Takahashi and Norio Yabuuchi, American Chemical Society, *LENRSB* 1 (2008) 57-8
- [26] Akito Takahashi, Proc. JCF-16, pp. 41-65, 2016